Journal of Peptide Science
*J. Peptide Sci.* **10**: 612–621 (2004)
Published online 7 April 2004 in Wiley InterScience (www.interscience.wiley.com). DOI: 10.1002/psc.570

JOURNAL OF PEPTIDE SCIENCE

# Interaction Between Amyloid β-Protein Aggregates and Membranes

**ATSUKO KAKIO,[a] YOSHIAKI YANO,[b] DENSHI TAKAI,[b] YUKIHIRO KURODA,[b] OSAMU MATSUMOTO,[b] YASUNORI KOZUTSUMI[c,d] and KATSUMI MATSUZAKI[b]***

[a] Department of Energy and Hydrocarbon Chemistry, Graduate School of Engineering, Kyoto University, Sakyo-ku, Kyoto 606-8501, Japan
[b] Graduate School of Pharmaceutical Sciences, Kyoto University, Sakyo-ku, Kyoto 606-8501, Japan
[c] Graduate School of Biostudies, Kyoto University, Sakyo-ku, Kyoto 606-8501, Japan
[d] Glyco-chain expression Laboratory, Supra-biomolecular System Research, RIKEN Frontier Research System, Wako 351-0198, Japan

*Received 15 December 2003*
*Accepted 22 January 2004*

Abstract: The conversion of soluble, nontoxic amyloid β-protein (Aβ) to aggregated, toxic Aβ rich in β-sheet structures is considered to be the key step in the development of Alzheimer's disease. Therefore, extensive studies have been carried out on the mechanisms involved in Aβ aggregation and the characterization of Aβ aggregates formed in aqueous solutions mimicking biological fluids. On the other hand, several investigators pointed out that membranes play an important role in Aβ aggregation. However, it remains unclear whether Aβ aggregates formed in solution and membranes are identical and whether the former can bind to membranes. In this study, using a dye-labeled Aβ-(1–40) as well as native Aβ-(1–40), the properties of Aβ aggregates formed in buffer and raft-like membranes composed of monosialoganglioside GM1/cholesterol/sphingomyelin were compared. Fourier transform infrared spectroscopic measurements suggested that Aβ aggregates formed in buffer and in membranes have different β-sheet structures. Fluorescence experiments revealed that Aβ aggregated in buffer did not show any affinity for membranes. 

Keywords: Alzheimer's disease; amyloid β-protein; aggregates; lipid raft; protein–membrane interaction

## INTRODUCTION

The conversion of soluble, nontoxic amyloid β-protein (Aβ) to aggregated, toxic Aβ rich in β-sheet structures is considered to be the key step in the development of Alzheimer's disease (AD) [1–3]. Therefore, extensive studies have been carried out on the mechanisms involved in Aβ aggregation, the characterization of Aβ aggregates, and the prevention of aggregate formation in aqueous solutions mimicking biological fluids. For example, Aβ has been shown spontaneously to form amyloid fibrils upon incubation of Aβ solution at 37 °C, but the concentration required for this ($>10^{-4}$–$10^{-5}$ M) [4–6] is much higher than the physiological concentration of Aβ in biological fluids ($<10^{-8}$ M) [7]. Seeded or nucleation-dependent polymerization has been hypothesized as an alternative mechanism that promotes Aβ aggregation even at a very low concentration [8]. The rate-limiting step of Aβ polymerization is the formation of an aggregation seed with a conformation that is characteristic of the

*Correspondence to: Prof. Katsumi Matsuzaki, Graduate School of Pharmaceutical Sciences, Kyoto University, Sakyo-ku, Kyoto 606-8501, Japan; e-mail: katsumim@pharm.kyoto-u.ac.jp
Contract/grant sponsor: Ministry of Education, Science, Sports and Culture, Japan; Contract/grant number: 15016058, 12140202.
Contract/grant sponsor: Ministry of Health, Labor and Welfare, Japan; Contract/grant number: 14A-1.

aggregate and is different from that of soluble Aβ. The seed or nucleus may assemble into protofibrils that finally grow into fibrils [9]. Recent solid-state NMR studies revealed that the fibrils are composed of in-resister parallel β-sheets [10–12]. Accumulating evidence suggests that the most neurotoxic species are not final fibrils but intermediates during fibril formation [13–18]. Low molecular weight compounds that inhibit Aβ aggregation also prevent Aβ neurotoxicity [19–21].

On the other hand, several investigators pointed out that membranes play an important role in Aβ aggregation. Yanagisawa *et al.* discovered monosialoganglioside GM1-bound Aβ (GM1-Aβ) in the brains of patients with AD and suggested that GM1-Aβ may act as a seed for Aβ polymerization [22,23]. Indeed, in human neuroblastoma cells, approximately half of detergent-insoluble Aβ was present in lipid rafts [24] rich in gangliosides, sphingomyelin (SM) and cholesterol [25]. Furthermore, gangliosides including GM1 [26–28] as well as oxidized phospholipids [29] have been shown to accelerate the rate of amyloid fibril formation of soluble Aβ *in vitro*. However, it remains unclear whether Aβ aggregates formed in solution and membranes are identical and whether the former can bind to membranes.

This study, using a dye-labeled Aβ-(1–40) as well as native Aβ-(1–40), comparatively investigated the properties of Aβ aggregates formed in buffer and raft-like membranes composed of GM1/cholesterol/SM. It was found that both aggregates differ in structure and that Aβ aggregates formed in buffer do not show membrane affinity.

## MATERIALS AND METHODS

### Peptides

Human Aβ-(1–40) labeled with a 7-diethylaminocoumarin-3-carbonyl group at the *N*-terminus (DAC-Aβ) was custom synthesized and characterized by the Peptide Institute (Minou, Japan). The dye-labeled peptide was always handled in light-protected, capped tubes under a nitrogen atmosphere to avoid photodegradation. Unlabeled human Aβ-(1–40) (HCl salt form) was also purchased from the Peptide Institute. The peptides were dissolved in 0.02% ammonia on ice, and any large aggregates that may act as polymerization seeds were removed by ultracentrifugation in 500 μl polyallomer tubes at 100 000 *g*, 4 °C for 3 h [30]. The peptide concentration of the supernatant was determined in triplicate by Micro BCA protein assay (Pierce, Rockford, IL). The supernatant, which contained only monomeric peptides [31], was collected and stored at −80 °C until use. Just before the experiment, the stock solution was thawed and mixed with an equal volume of double concentrated buffer (20 mM Tris/300 mM NaCl/2 mM EDTA or 4 mM $CaCl_2$, pH 7.4).

### Preparation of Lipid Vesicles

Egg yolk-L-α-phosphatidylcholine (PC) and cholesterol were purchased from Sigma (St Louis, MO). GM1 was obtained from Avanti (Alabaster, AL). Bovine brain SM was purchased from Matreya (Pleasant Gap, PA).

Large unilamellar vesicles (LUVs) were prepared and characterized as follows. Lipids were first mixed in a chloroform–methanol 2 : 1 (v/v) mixture and the solvent was removed by evaporation in a rotary evaporator. The residual lipid film, after drying under vacuum overnight, was hydrated with buffer (10 mM Tris/150 mM NaCl/2 mM $CaCl_2$, pH 7.4) and vortex mixed to produce multilamellar vesicles (MLVs). The suspension was subjected to five cycles of freezing and thawing, and then extruded through polycarbonate filters (100 nm pore size filter, 31 times) using a Liposofast extruder (Avestin, Ottawa, Canada). The lipid concentration was determined in triplicate by a phosphorus analysis [32].

Small unilamellar vesicles (SUVs) for Fourier transform infrared-attenuated total reflection (FTIR-ATR) experiments were prepared by sonication of MLVs under a nitrogen atmosphere for 15 min (5 min × 3 times) using a probe-type sonicator. $CaCl_2$ in the buffer was replaced with 1 mM EDTA because the calcium ion interferes with the fibril formation. Metal debris from the titanium tip of the probe was removed by centrifugation.

### Preparation and Characterization of Aggregated DAC-Aβ

DAC-Aβ (100 μM) dissolved in buffer (10 mM Tris/150 mM NaCl/1 mM EDTA, pH 7.4) was incubated for 0, 4, 8 and 48 h at 37 °C. The fibril formation of DAC-Aβ was confirmed by atomic force microscopy (AFM). The samples diluted to 0.1 μM were deposited on freshly cleaved mica, washed within a few seconds with water, dried in a laminar-flow hood for 60 min. The specimens were imaged using a multimode AFM and a NanoScope IIIa controller (Digital

Instruments, Santa Barbara, CA) in tapping mode using silicon nitride probes with a nominal spring constant of 0.32 N/m. The drive frequency and amplitude were 8–9 kHz and 1–20 nm, respectively. The scan rate was 0.5 Hz.

### Fluorescence

Fluorescence emission spectra of DAC-A$\beta$ were recorded under stirring at an excitation wavelength of 430 nm on a Shimadzu RF-5000 spectrofluorometer. The temperature of the cuvette holder was controlled at $37^\circ \pm 0.5\,^\circ$C. The reported spectra were the averaged spectra for two independent samples after subtraction of the corresponding blank spectra (buffer or LUVs) and volume correction for titration experiments.

### FTIR-ATR Measurements

To investigate the secondary structures of aggregated A$\beta$s formed in the solution and membranes, FTIR-ATR measurements were made. The HCl salt form of native human A$\beta$-(1–40) was used because the strong band around 1673 $cm^{-1}$ due to the conventionally used trifluoroacetate salt overlaps the amide I band [33]. Two types of aggregated A$\beta$s were prepared as follows. A$\beta$ aggregated in solution was prepared by incubating A$\beta$-(1–40) (30 $\mu$M) at 37 °C for 24 h. The aggregates were collected by ultracentrifugation in 500 µl polyallomer tubes at 100 000 *g* and 4 °C for 3 h. The pellets were washed twice with water to remove the buffer components.

Care should be taken when preparing aggregated A$\beta$ in raft-like membranes. The HCl salt form of A$\beta$ is known to easily self-aggregate even without the addition of a polymerization seed [34]. Preliminary experiments using the Thioflavin T (ThT) assay showed that the incubation period should be shorter than 4 h to avoid spontaneous fibril formation in the aqueous phase even at a lower concentration of 15 $\mu$M. To facilitate fibril formation in the presence of raft-like membranes during a short incubation period, the GM1 content was increased and SUVs were used with a larger specific surface area. Thus, A$\beta$-(1–40) (15 $\mu$M) was incubated with 450 $\mu$M raft-like SUVs composed of GM1/cholesterol/SM (1/1/1) at 37 °C for 2 h. A GM1-to-A$\beta$ ratio of 10 was optimal for fibril formation [28]. Fibril formation was confirmed to start without a lag time after the mixing of the protein with the membranes by the ThT assay (Hayashi *et al.*, unpublished work). After the incubation, aggregated A$\beta$ was precipitated by ultracentrifugation as described above.

The two types of aggregated A$\beta$s were subjected to FTIR-ATR measurements. Dry films of aggregated A$\beta$s were prepared by spreading the pellets on a germanium ATR plate ($80 \times 10 \times 4$ mm) followed by gradual evaporation of water. The last traces of water were removed by use of $P_2O_5$ under vacuum overnight. To minimize the atmospheric water vapor, the instrument was purged with dry $N_2$ gas. FTIR-ATR measurements were carried out on a BioRad FTS-3000MX spectrometer equipped with an Hg–Cd–Te detector and a PIKE horizontal ATR attachment. The total reflection number was 10 on the film side. The spectra were measured at a resolution of 2 $cm^{-1}$ and an angle of incidence of 45°, and derived from 256 co-added interferograms with the Happ-Genzel apodization function. Subtraction of the gently sloping water vapor was carried out to improve the background prior to frequency measurement. For ATR correction, refractive indexes of 4.003, 1.7, 1.57 and 1.44 were used for germanium, A$\beta$, A$\beta$ with raft-like membranes, and raft-like membranes, respectively [35].

## RESULTS

### Secondary Structures of Aggregated A$\beta$s Formed in Solution and Raft-like Membranes

Figure 1 shows FTIR-ATR spectra in the region of 1500–1700 $cm^{-1}$ of aggregated A$\beta$s formed in buffer (A and C) and raft-like membranes (B and D). The dotted traces in B and D represent the reference spectra of raft-like membranes only.

In the amide I region 1600–1700 $cm^{-1}$, the spectrum of A$\beta$ aggregated in buffer (Figure 1A) showed an intensive band at 1629 $cm^{-1}$, a small absorption around 1660 $cm^{-1}$, and a faint shoulder at ~1695 $cm^{-1}$. On the other hand, A$\beta$ aggregated in raft-like membranes showed a different spectrum (Figure 1B). Comparison of the A$\beta$ spectrum (solid trace) with that of the raft membranes only (dotted trace) revealed that strong 1633 and weak 1695 $cm^{-1}$ bands were assigned to A$\beta$. The intensity of the band at 1695 $cm^{-1}$ relative to that of the strongest band around 1630 $cm^{-1}$ was larger than that in Figure 1A, taking the contribution from the membranes into account. In contrast to Figure 1A, no conspicuous band was detected around 1660 $cm^{-1}$.

In the amide II region, spectral differences were also observed between the two types of

 

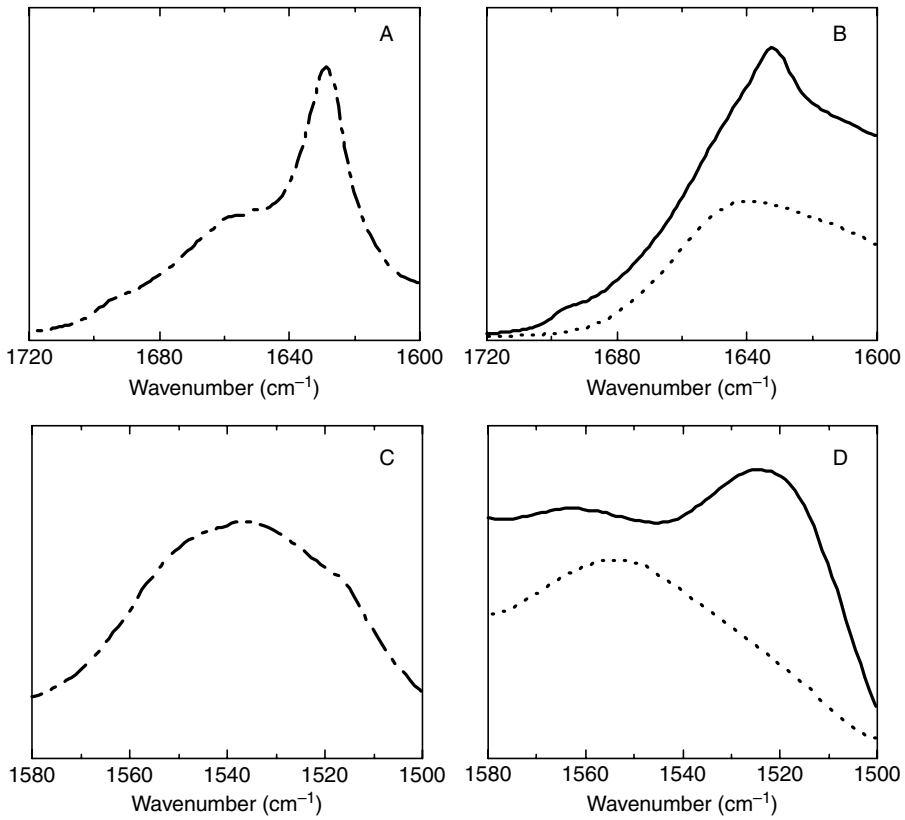


Figure 1 FTIR-ATR spectra of aggregated Aβs formed in buffer (A and C, dashed traces) and raft-like membranes composed of GM1/cholesterol/SM (1/1/1) (B and D, solid traces). The dotted traces (B and D) represent the reference spectra of raft-like membranes only.

aggregated Aβs (Figures 1C and D). Aβ aggregated in solution (Figure 1C) showed a broad absorption band centered at 1537 cm$^{-1}$, whereas Aβ aggregated in the membranes (Figure 1D, solid trace) showed a strong band at 1524 cm$^{-1}$. The raft-like membranes (Figure 1D, dotted trace) exhibited an absorption band around 1555 cm$^{-1}$, which was far apart from the peak of the Aβ aggregated in the membranes.

## DAC-Aβ Aggregated in Aqueous Solution

DAC-Aβ (100 μM) dissolved in buffer was preincubated for various periods at 37 °C. The fluorescence spectra of the incubated samples were measured after an immediate dilution to 0.5 μM (Figure 2A). The fluorescence intensity was decreased with an increase in incubation time. At the same time, a shoulder appeared around 520 nm.

The aggregate formation was confirmed by AFM. Figure 2B shows an AFM image of a 24 h incubated peptide as an example. The aggregates were morphologically very similar to those reported for the native Aβ [36]. It was reported that DAC-Aβ shows the same lipid specificity as the native protein [31]. Thus, the dye-labeled protein behaves, at least qualitatively, very similarly to the native protein.

## Fluorescence Spectra of DAC-Aβ Incubated with Raft-like Membranes

Monomeric DAC-Aβ was incubated with raft-like membranes composed of GM1/cholesterol/SM (2/4/4) at 37 °C. A lipid-to-DAC-Aβ ratio of 1960 used here corresponds to a local protein concentration of ca. 120 μM, assuming 50% membrane binding (as judged from the fluorescence intensity [28]), an average area per lipid of 0.5 nm$^2$ and a membrane thickness of 7 nm.[†] Prolonged incubation

[†] Monolayer studies indicated that GM1, cholesterol and SM occupy areas per molecule of 0.75 [56], 0.35 and 0.51 [57] nm$^2$ at surface pressures corresponding to bilayers. The averaged area per lipid of the raft-like membranes composed of GM1/cholesterol/SM (2/4/4) was calculated to be 0.5 nm$^2$. The thickness of GM1-containing bilayers at 37 °C was estimated to be 7 nm based on a recent structural study [58].

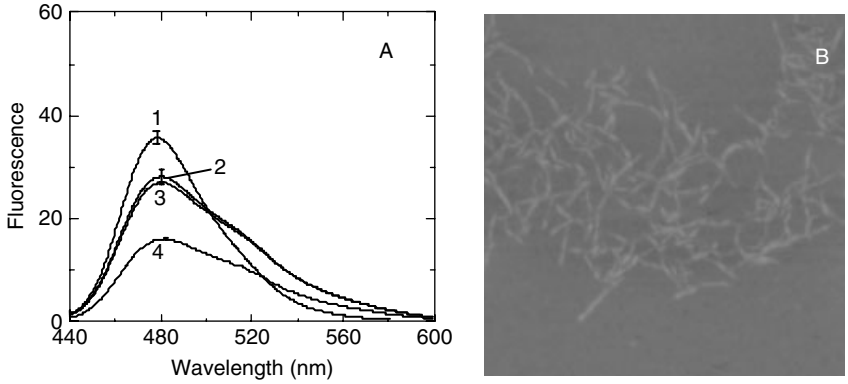


Figure 2 DAC-A$\beta$ aggregated in aqueous solution. DAC-A$\beta$ (100 μM) in 10 mM Tris/150 mM NaCl/1 mM EDTA buffer (pH 7.4) was incubated at 37 °C for different periods. (A) Immediately after dilution to 0.5 μM, fluorescence spectra at the same temperature were recorded at an excitation wavelength of 430 nm. Traces 1–4 correspond to 0, 4, 8 and 48 h incubation, respectively. Standard deviations at the peaks are shown by error bars ($n = 2$). (B) The sample after 24 h incubation was mounted for AFM analysis at 0.1 μM. Representative 1 × 1 μm x-y, 10 nm total z-range AFM image is shown.

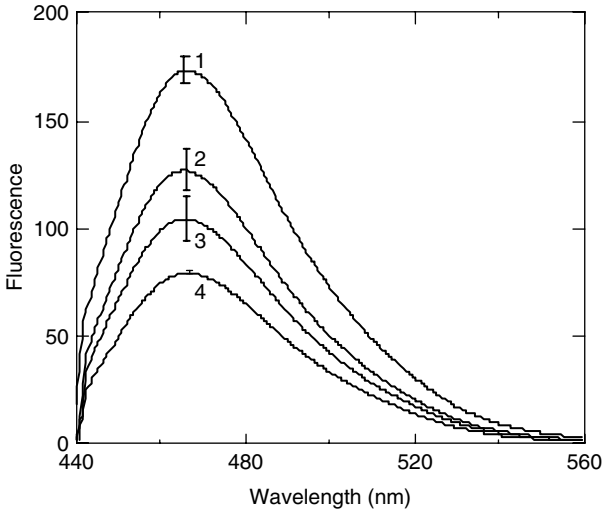


Figure 3 Fluorescence spectra of DAC-A$\beta$ incubated with raft-like membranes. DAC-A$\beta$ (0.5 μM) was incubated with 980 μM LUVs composed of GM1/cholesterol/SM (2/4/4) at 37 °C for different periods. Traces 1–4 correspond to 0, 1, 2 and 3 d incubation, respectively. Standard deviations at the peaks are shown by error bars ($n = 2$).

at this high local concentration time-dependently reduced the fluorescence intensity without changing the spectral shape (Figure 3).

## Membrane Binding Properties of DAC-A$\beta$ Aggregated in Aqueous Solution

The aggregational state of A$\beta$ may affect its membrane affinity. The binding of aggregated DAC-A$\beta$ to raft-like membranes was investigated in comparison with that of monomeric DAC-A$\beta$ (Figure 4). DAC-A$\beta$(100 μM) was preincubated at 37 °C for 0, 4, 8 and 48 h. Immediately after dilution to 0.5 μM, the protein solutions were titrated with raft-like LUVs composed of GM1/cholesterol/SM (2/4/4), and fluorescence spectra were recorded. Addition of raft-like LUVs to monomeric DAC-A$\beta$ enhanced the fluorescence intensity of DAC accompanied with a blue shift in the emission maximum (from 478 to 466 nm), indicating a change in polarity upon membrane binding [31]. In contrast, DAC-A$\beta$ preincubated for 4 and 8 h showed smaller fluorescence increases upon LUV addition (Figures 4B and C). It should be noted that the fluorescence spectra with the membranes showed no shoulder around 520 nm, which was characteristic of DAC-A$\beta$ aggregated in solution. Extensively aggregated DAC-A$\beta$ after a 48 h preincubation exhibited extremely suppressed fluorescence enhancements upon LUV addition (Figure 4D).

The titration interval in Figure 4 was 3 min, which was confirmed to be sufficient for the membrane binding of monomeric DAC-A$\beta$ [37]. However, since A$\beta$ aggregation is a reversible process [38,39], a much longer incubation may increase membrane binding by monomer molecules generated from the disassociation of aggregates. Figure 5 shows the effects of postincubation on the binding of aggregated DAC-A$\beta$ to raft-like membranes. The samples at a lipid-to-protein ratio of 1960 in Figure 4 were further incubated (postincubated) at 37 °C for long periods. The sample without preincubation (trace 1) exhibited a continuous

 

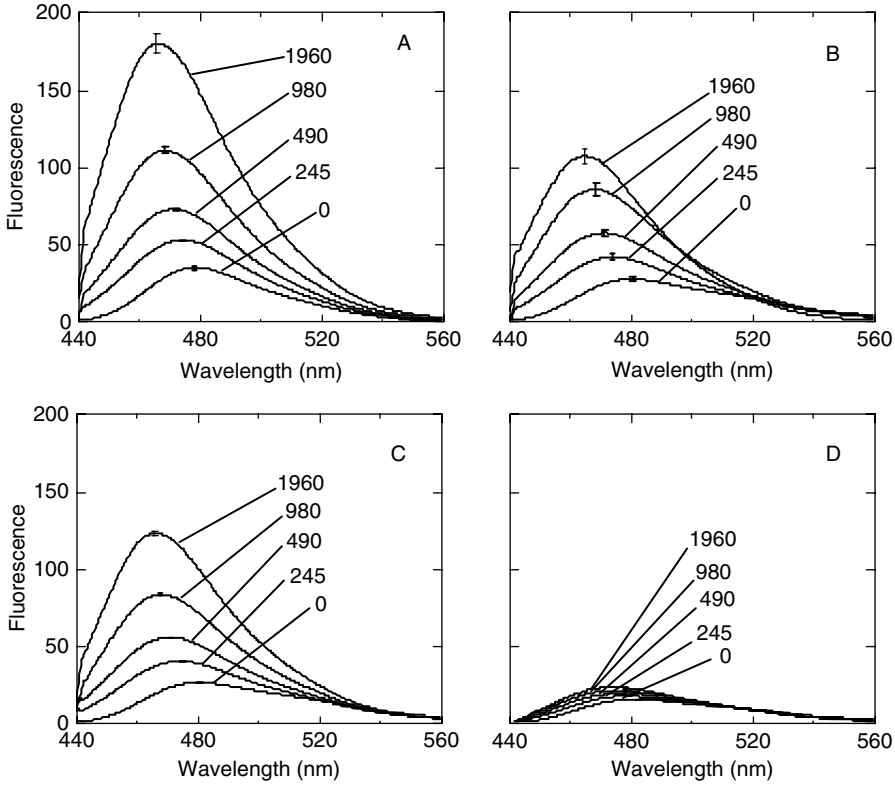


Figure 4 Binding of aggregated DAC-Aβ to raft-like membranes at 37 °C. DAC-Aβ (100 μM) in 10 mM Tris/150 mM NaCl/1 mM EDTA buffer (pH 7.4) was preincubated at 37 °C for (A) 0, (B) 4, (C) 8 and (D) 48 h. Immediately after dilution to 0.5 μM, the protein solutions were titrated with raft-like LUVs composed of GM1/cholesterol/SM (2/4/4) and fluorescence spectra were recorded at an excitation wavelength of 430 nm. The numbers in the figure represent lipid-to-DAC-Aβ ratios. Standard deviations at the peaks are shown by error bars ($n = 2$).

decrease in fluorescence during postincubation, as shown in Figure 3. In contrast, the samples with DAC-Aβ preincubated for 4 and 8 h (traces 2 and 3) behaved differently. The fluorescence intensities first increased to levels almost identical to that of trace 1, and then decreased similarly to trace 1 after 1 day. The sample with DAC-Aβ preincubated for 48 h (trace 4) exhibited a similar biphasic behavior, but the level of fluorescence was significantly lower than those of traces 2 and 3.

Monomeric DAC-Aβ is known to specifically bind to membranes containing a ganglioside cluster and to show no affinity for other classes of lipids [28,31]. Aggregated DAC-Aβ might possess a different lipid specificity. The binding of DAC-Aβ with various aggregational states to LUVs of different lipid compositions was examined based on DAC fluorescence (Figure 6). All samples showed a selective affinity for raft-like membranes.

## DISCUSSION

### Structures of Aβs Aggregated in Solution and Membranes

Recent solid-state NMR studies concluded that the fibrils formed in solution are composed of in-resister parallel β-sheets with the disordered *N*-terminal region and a turn formed by residues 25–29 [10–12]. Our FTIR and fluorescence spectra support this conclusion. The appearance of the major band at 1629 $cm^{-1}$ (Figure 1A) indicates that the aggregated Aβ-(1–40) protein assumes a β-sheet structure with a stronger interchain interaction. The small band around 1660 $cm^{-1}$ can be assigned to the disordered *N*-terminal region and/or the central turn. The parallel β-sheet formation allows close dye–dye contacts, which affect the electronic state of the DAC moiety, resulting in the appearance of a shoulder around 520 nm in fluorescence spectra (Figure 2A) [40]. A reduction in fluorescence intensity also indicates the aggregate formation,

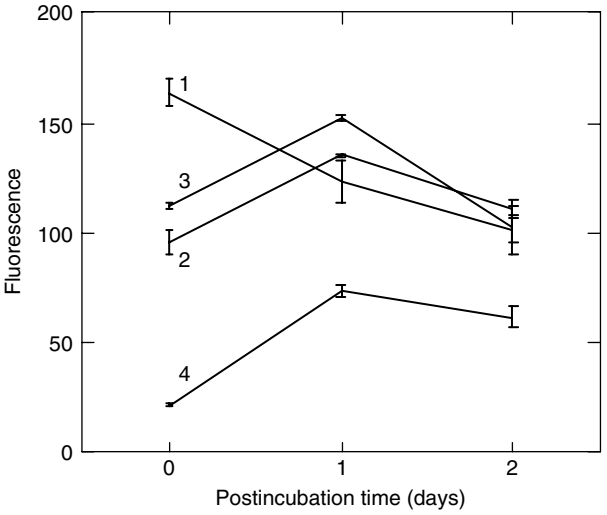


Figure 5 Effects of postincubation on the binding of aggregated DAC-A$\beta$ to raft-like membranes. The samples at a lipid-to-DAC-A$\beta$ ratio of 1960 in Figure 4 were further incubated at 37 °C. Traces 1–4 correspond to preincubation periods of 0, 4, 8 and 48 h, respectively. Fluorescence intensities at 470 nm (excitation at 430 nm) are plotted as a function of the postincubation time. Standard deviations are shown by error bars ($n = 2$).

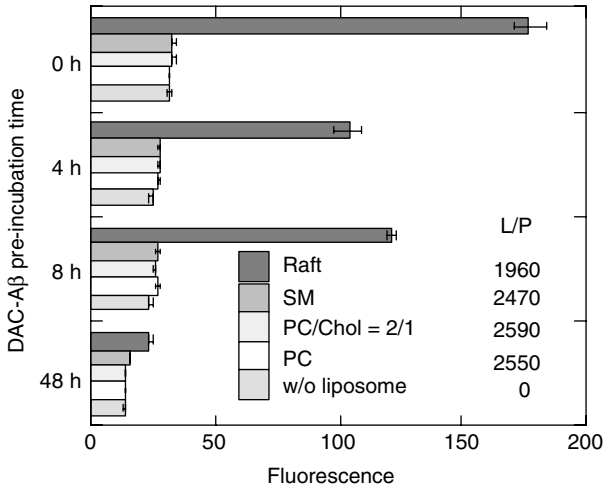


Figure 6 Binding of aggregated DAC-A$\beta$ to various lipids at 37 °C. DAC-A$\beta$ (100 μM) in 10 mM Tris/150 mM NaCl/1 mM EDTA buffer (pH 7.4) was preincubated at 37 °C for 0, 4, 8 and 48 h. Immediately after dilution to 0.5 μM, the protein solutions were mixed with various LUVs composed of raft-like GM1/cholesterol/SM (2/4/4), SM, PC/cholesterol (2/1) and PC at lipid-to-DAC-A$\beta$ ratios (L/P) indicated in the figure. Fluorescence intensities at 470 nm (excitation at 430 nm) are summarized. Standard deviations are shown by error bars ($n = 2$). Fluorescence intensities without membranes are also included as a reference.

which can reduce light absorption due to the hypochromic [40] as well as flattening effects [41]. The introduction of the DAC moiety at the *N*-terminus did not inhibit fibril formation (Figure 2B) because of the disordered *N*-terminal region.

The structure of A$\beta$ aggregates formed in raft-like membranes appears to be not identical to that in solution. Amide I region FTIR data (Figure 1B) showed the higher wavenumber of the major band (1633 $cm^{-1}$) and the coappearance of the weak band around 1690 $cm^{-1}$. The former suggests the aggregates adopt $\beta$-sheets with weaker interchain interactions. The latter band was previously considered to be a hallmark of antiparallel $\beta$-sheets [42,43]. However, A$\beta$s, which form parallel $\beta$-sheets in aqueous solution, were also reported to show this weak band [4,10,44]. Our aggregates formed in solution showed only a faint band in this wavelength region (Figure 1A). Limited information is available on the relationship between secondary structures and amide II band positions [43,45]. $\beta$-Sheets show a strong absorption band around 1530 $cm^{-1}$, as observed for both aggregates (Figures 1 C and D). The coappearance of a weak band around 1550 $cm^{-1}$ is suggested to be a hallmark of parallel $\beta$-sheets [43]. The aggregates formed in solution exhibited this, although random structures also show bands in this region [45]. Anyway, the different amide II spectra suggest that both types of aggregates assume nonidentical conformations. The driving force of fibril formation in aqueous phase is considered to be hydrophobic interactions between closely contacted hydrophobic side chains [12]. In the membrane phase, however, the hydrophobic amino acids can also interact with lipids. Therefore, there is no need for both $\beta$-sheets to adopt the identical structure. To definitely determine the structure of membrane-aggregated A$\beta$, further studies such as solid-state NMR are required.

The group of Mantsch measured the FTIR spectra of amyloid deposits *in situ* in the AD brain [46]. The amide I band was characterized by an intense peak at 1631 $cm^{-1}$ and a shoulder around 1650 $cm^{-1}$ without a discernible band around 1690 $cm^{-1}$. The amide II band showed a peak at 1540 $cm^{-1}$ and a shoulder 1519 $cm^{-1}$. Therefore, amyloid deposits in the AD brain assume secondary structures closer to those of A$\beta$ aggregated in solution, although the deposits may contain proteins other than A$\beta$.

Fluorescence data may also suggest the nonidentity of both types of aggregates. The preincubation of

 

DAC-Aβ with raft-like membranes only reduced the fluorescence intensity without any spectral shape change (Figure 3). A straightforward interpretation of these findings would be that the fluorescence was self-quenched because of self-aggregation, as observed for the fluorescein-labeled Aβ [37], and that the DAC moieties were not so close to each other as to allow electronic interactions. The self-quenching technique has been often used to monitor protein aggregation [47,48]. However, the possibility cannot be excluded that this time-dependent fluorescence decrease is partially due to a chemical degradation of the dye and/or adsorption of the protein to containers.

### Interactions of Aβ Aggregates with Membrane

A number of studies have been published on Aβ–membrane interactions. There are some discrepancies among the results by different research groups. For example, no interaction with zwitterionic PC liposomes [31,49,50] was observed for Aβ-(1–40) and DAC-Aβ, whereas some studies reported that Aβ-(1–40) and Aβ-(1–42) interacted with PC liposomes [51,52]. One reason for this may be the different solution states of Aβ. Indeed, aggregated but not freshly solubilized Aβ was found to interact with and decrease the fluidity of PC bilayers [53]. Selective affinity of cholesterol, fatty acids and PC for aggregated Aβ-(1–40) was also reported [54]. However, this study clearly shows that the aggregation inhibits the binding of DAC-Aβ to raft-like membranes (Figure 4) and does not allow the protein to bind to lipids other than ganglioside clusters (Figure 6), although the reason for the discrepancy between this and previous studies is not clear. The peptide concentration may be a factor affecting protein–membrane interaction. Furthermore, commercially available Aβ may contain nontrivial amounts of impurities [55]. Importantly, the fact that the fluorescence spectra of aggregated DAC-Aβ in the presence of raft-like membranes showed no shoulder around 520 nm (Figure 4) suggests that only monomeric protein can bind to the membrane. This hypothesis is supported by the observations that postincubation of aggregated DAC-Aβ–membrane mixtures enhanced membrane binding (Figure 5). The system appears to reach a new equilibrium state at least after 1 day regardless of the initial aggregational state, as long as the initial aggregation is not so extensive. The dock–lock mechanism for fibril formation [38] can explain why the 48 h preincubated DAC-Aβ showed significantly reduced membrane binding even after a long postincubation: prolonged incubation of Aβ in solution increases the fraction of the 'locked' protein that cannot dissociate into soluble monomer.

## REFERENCES


1. Selkoe DJ. Cell biology of the amyloid β-protein precursor and the mechanism of Alzheimer's disease. *Annu. Rev. Cell Biol.* 1994; **10**: 373–403.
2. Harper JD, Lansbury PT Jr. Models of amyloid seeding in Alzheimer's disease and scrapie: mechanistic truths and physiological consequences of the time-dependent solubility of amyloid proteins. *Annu. Rev. Biochem.* 1997; **66**: 385–407.
3. Lansbury PT Jr. Structural neurology: are seeds at the root of neuronal degeneration? *Neuron* 1997; **19**: 1151–1154.
4. Fraser PE, Nguyen JT, Inoue H, Surewicz WK, Selkoe DJ, Podlinski MB, Kirschner DA. Fibril formation by primate, rodent, and Dutch-hemorrhagic analogues of Alzheimer amyloid β-protein. *Biochemistry* 1992; **31**: 10 716–10 723.
5. Walsh DM, Lomakin A, Benedek GB, Condron MM, Teplow DB. Amyloid β-protein fibrillogenesis. Detection of a protofibrillar intermediate. *J. Biol. Chem.* 1997; **272**: 22 364–22 372.
6. Naiki H, Gejyo F. Kinetic analysis of amyloid fibril formation. *Methods Enzymol.* 1999; **309**: 305–318.
7. Seubert P, Vigo-Pelfrey C, Esch F, Lee M, Dovey H, Davis D, Sinha S, Schlossmacher M, Whaley J, Swindlehurst C, McCormack R, Wolfert R, Selkoe J, Lieberburg I, Schenk D. Isolation and quantification of soluble Alzheimer's β-peptide from biological fluids. *Nature* 1992; **359**: 325–327.
8. Jarrett JT, Lansbury Jr PT. Seeding 'one-dimensional crystallization' of amyloid: a pathogenic mechanism in Alzheimer's disease and scrapie? *Cell* 1993; **73**: 1055–1058.
9. Bitan G, Kirkitadze MD, Lomakin A, Vollers SS, Benedek GB, Teplow DB. Amyloid β-protein (Aβ) assembly: Aβ40 and Aβ42 oligomerize through distinct pathways. *Proc. Natl Acad. Sci. USA* 2003; **100**: 330–335.
10. Antzukin ON, Balbach JJ, Leapman RD, Rizzo NW, Reed J, Tycko R. Multiple quantum solid-state NMR indicates a parallel, not antiparallel, organization of β-sheets in Alzheimer's β-amyloid fibrils. *Proc. Natl Acad. Sci. USA* 2000; **97**: 13 045–13 050.
11. Balbach JJ, Petkova AT, Oyler NA, Antzukin ON, Gordon DJ, Meredith SC, Tycko R. Supramolecular structure in full-length Alzheimer's β-amyloid fibrils: Evidence for a parallel β-sheet organization from solid-state nuclear magnetic resonance. *Biophys. J.* 2002; **83**: 1205–1216.

12. Petkova AT, Ishii Y, Balbach JJ, Antzukin ON, Leapman RD, Delaglio F, Tycko R. A structural model for Alzheimer's $\beta$-amyloid fibrils based on experimental constrains from solid state NMR. *Proc. Natl Acad. Sci. USA* 2002; **99**: 16 742–16 747.
13. Lambert MP, Barlow AK, Chromy BA, Edwards C, Freed R, Liosatos M, Morgan TE, Rozovsky I, Trommer B, Viola KL, Wals P, Zhang C, Finch CE, Krafft GA, Klein WL. Diffusible, nonfibrillar ligands derived from $A\beta_{1-42}$ are potent central nervous system neurotoxins. *Proc. Natl Acad. Sci. USA* 1998; **95**: 6448–6453.
14. Hartley DM, Walsh DM, Ye CP, Diehl T, Vasquez S, Vassilev PM, Teplow DB, Selkoe DJ. Protofibrillar intermediates of amyloid $\beta$-protein induce acute electrophysiological changes and progressive neurotoxicity in cortical neurons. *J. Neurosci.* 1999; **19**: 8876–8884.
15. Walsh DM, Kyubin I, Fadeeva JV, Cullen WK, Anwyl R, Wolfe MS, Rowan MJ, Selkoe DJ. Naturally secreted oligomers of amyloid $\beta$ protein potently inhibit hippocampal long-term potentiation *in vivo*. *Nature* 2002; **416**: 535–539.
16. Dahlgren KN, Manelli AM, Stine JWB, Baker LK, Krafft GA, LaDu MJ. Oligomeric and fibrillar species of amyloid-$\beta$ peptides differentially affect neuronal viability. *J. Biol. Chem.* 2002; **277**: 32 046–32 053.
17. Hoshi M, Sato M, Matsumoto S, Nogichi A, Yasutake K, Yoshida N, Sato K. Spherical aggregates of $\beta$-amyloid (amylospheroid) show high neurotoxicity and activate tau protein kinase I/glycogen synthase kinase-3$\beta$. *Proc. Natl Acad. Sci. USA* 2003; **100**: 6370–6375.
18. Kayed R, Head E, Thompson JL, McIntire TM, Milton SC, Cotman CW, Glable CG. Common structure of soluble amyloid oligomers implies common mechanism of pathogenesis. *Science* 2003; **300**: 486–489.
19. Salomon AR, Marcinowski KJ, Friedland RP, Zagorski MG. Nicotine inhibits amyloid formation by the $\beta$-peptide. *Biochemistry* 1996; **35**: 13 568–13 578.
20. Tomomiya T, Shoji A, Kataoka K, Suwa Y, Asano S, Kaneko H, Endo N. Inhibition of amyloid $\beta$ protein aggregation and neurotoxicity by rifampicin. *J. Biol. Chem.* 1996; **271**: 6839–6844.
21. Lowe TL, Strzelec A, Kiessling LL, Murphy RM. Structure–function relationships for inhibitors of $\beta$-amyloid toxicity containing the recognition sequence KLVFF. *Biochemistry* 2001; **40**: 7882–7889.
22. Yanagisawa K, Odaka A, Suzuki N, Ihara Y. GM1 ganglioside-bound amyloid $\beta$-protein (A$\beta$): a possible form of preamyloid in Alzheimer's disease. *Nat. Med.* 1995; **1**: 1062–1066.
23. Yanagisawa K, Ihara Y. GM1 ganglioside-bound amyloid $\beta$-protein in Alzheimer's disease brain. *Neurobiol. Aging* 1998; **19**: S65–S67.
24. Morishima-Kawashima M, Ihara Y. The presence of amyloid $\beta$-protein in the detergent-insoluble membrane compartment of neuroblastoma cells. *Biochemistry* 1998; **37**: 15 247–15 235.
25. Simons K, Ikonen E. Functional rafts in cell membranes. *Nature* 1997; **385**: 569–572.
26. ChooSmith L-P, Garzon-Rodriguez W, Glabe CG, Surewicz WK. Acceleration of amyloid fibril formation by specific binding of A$\beta$-(1–40) peptide to ganglioside-containing membrane vesicles. *J. Biol. Chem.* 1997; **272**: 22 987–22 990.
27. McLaurin J, Franklin T, Fraser PE, Chakrabartty A. Structural transitions associated with the interaction of Alzheimer $\beta$-amyloid peptides with gangliosides. *J. Biol. Chem.* 1998; **273**: 4506–4515.
28. Kakio A, Nishimoto S, Yanagisawa K, Kozutsumi Y, Matsuzaki K. Interactions of amyloid $\beta$-protein with various gangliosides in raft-like membranes: Importance of GM1 ganglioside-bound form as an endogenous seed for Alzheimer amyloid. *Biochemistry* 2002; **41**: 7385–7390.
29. Koppaka V, Axelsen PH. Accelerated accumulation of amyloid $\beta$ proteins on oxidatively damaged lipid membranes. *Biochemistry* 2000; **39**: 10 011–10 016.
30. Hasegawa K, Yamaguchi I, Omata S, Gejyo F, Naiki H. Interactions between A$\beta$(1–42) and A$\beta$(1–40) in Alzheimer's $\beta$-amyloid fibril formation *in vitro*. *Biochemistry* 1999; **38**: 15 514–15 521.
31. Kakio A, Nishimoto S, Yanagisawa K, Kozutsumi Y, Matsuzaki K. Cholesterol-dependent formation of GM1 ganglioside-bound amyloid $\beta$-protein, an endogenous seed for Alzheimer amyloid. *J. Biol. Chem.* 2001; **276**: 24 985–24 990.
32. Bartlett GR. Phosphorus assay in column chromatography. *J. Biol. Chem.* 1959; **234**: 466–468.
33. Surewicz WK, Mantsch HH. The conformation of dynorphin A-(1–13) in aqueous solution as studied by Fourier transform infrared spectroscopy. *J. Mol. Struct.* 1989; **214**: 143–147.
34. Kaneko I, Tutumi S. Replies to the editor. *J. Neurochem.* 1997; **68**: 438–439.
35. Goormaghtigh E, Raussens V, Ruysschaert J-M. Attenuated total reflection infrared spectroscopy of proteins and lipids in biological membranes. *Biochim. Biophys. Acta* 1999; **1422**: 105–185.
36. Stine JWB, Dahlgren KN, Krafft GA, LaDu MJ. *In vitro* characterization of conditions for amyloid-$\beta$ peptide oligomerization and fibrillogenesis. *J. Biol. Chem.* 2003; **278**: 11 612–11 622.
37. Kakio A, Nishimoto S, Kozutsumi Y, Matsuzaki K. Formation of a membrane-active form of amyloid $\beta$-protein in raft-like membranes. *Biochem. Biophys. Res. Commun.* 2003; **303**: 514–518.
38. Esler WP, Stimson ER, Jennings JM, Vinters HV, Ghilardi JR, Lee JP, Mantyh PW, Maggio JE. Alzheimer's disease amyloid propagation by a template-dependent dock-lock mechanism. *Biochemistry* 2000; **39**: 6288–6295.
39. Hasegawa K, Ono K, Yamada M, Naiki H. Kinetic modeling and determination of reaction constants of Alzheimer's $\beta$-amyloid fibril extension and dissociation

 

using surface plasmon resonance. *Biochemistry* 2002; **41**: 13 489–13 498.
40. Cantor CR, Schimmel PR. 1980; *Biophysical Chemistry*. W. H. Freeman and Co.: New York, 385–405.
41. Duysens LNM. The flattening of the absorption spectrum of suspensions, as compared to that of solutions. *Biochim. Biophys. Acta* 1956; **19**: 1–12.
42. Miyazawa T. Perturbation treatment of the characteristic vibrations of polypeptide chains in various configurations. *J. Chem. Phys.* 1960; **32**: 1647–1652.
43. Miyazawa T, Blout ER. The infrared spectra of polypeptides in various conformations: amide I and II bands. *J. Am. Chem. Soc.* 1961; **83**: 712–719.
44. Hilbich C, Kisters-Woike B, Reed J, Masters CL, Beyreuter K. Aggregation and secondary structure of synthetic amyloid βA4 peptides of Alzheimer's disease. *J. Mol. Biol.* 1991; **218**: 149–163.
45. Venyaminov SY, Kalnin NN. Quantitative IR spectrophotometry of peptide compounds in water ($H_2O$) solutions. II. Amide absorption bands of polypeptides and fibrous proteins in α-,β-, and random coil conformations. *Biopolymers* 1990; **30**: 1259–1271.
46. Choo L-P, Wetzel DL, Halliday WC, Jackson M, LeVine SM, Mantsch HH. *In situ* characterization of β-amyloid in Alzheimer's diseased tissue by synchrotron Fourier transform infrared microspectroscopy. *Biophys. J.* 1996; **71**: 1672–1679.
47. Runnels LW, Scarlata SF. Theory and application of fluorescence homotransfer to melittin oligomerization. *Biophys. J.* 1995; **69**: 1569–1583.
48. Wendt H, Berger C, Baici A, Thomas RM, Bosshard HR. Kinetics of folding of leucine zipper domains. *Biochemistry* 1995; **34**: 4097–4107.
49. Terzi E, Hölzmann G, Seelig J. Self-association of β-amyloid peptide (1–40) in solution and binding to lipid membranes. *J. Mol. Biol.* 1995; **252**: 633–642.
50. Matsuzaki K, Horikiri C. Interactions of amyloid β-peptide (1–40) with ganglioside-containing membranes. *Biochemistry* 1999; **38**: 4137–4142.
51. Mason RP, Jacob RF, Walter MF, Mason PE, Avdulov NA, Chochina SV, Igbavboa U, Wood WG. Distribution and fluidizing action of soluble and aggregated amyloid β-peptide in rat synaptic plasma membranes. *J. Biol. Chem.* 1999; **274**: 18 801–18 807.
52. Ji S-R, Wu Y, Sui S-F. Cholesterol is an important factor affecting the membrane insertion of β-amyloid peptide (Aβ1–40), which may potentially inhibit the fibril formation. *J. Biol. Chem.* 2002; **277**: 6273–6279.
53. Kremer JJ, Pallitto MM, Sklansky DJ, Murphy RM. Correlation of β-amyloid aggregate size and hydrophobicity with decreased bilayer fluidity of model membranes. *Biochemistry* 2000; **39**: 10 309–10 318.
54. Avdulov NA, Chochina SV, Igbavboa U, Warden CS, Vassiliev AV, Wood WG. Lipid binding to amyloid β-peptide aggregates: Preferential binding of cholesterol as compared with phosphatidylcholine and fatty acids. *J. Neurochem.* 1997; **69**: 1746–1752.
55. Fukuda H, Shimizu T, Nakajima M, Mori H, Shirasawa T. Synthesis, aggregation, and neurotoxicity of the Alzheimer's Aβ1–42 amyloid peptide and its isoaspartyl isomers. *Bioorg. Med. Chem. Lett.* 1999; **9**: 953–956.
56. Maggio B, Cumar FA, Caputto R. Molecular behaviour of glycosphingolipids in interfaces. Possible participation in some properties of native membranes. *Biochim. Biophys. Acta* 1981; **650**: 69–87.
57. Shaikh SR, Dumaual AC, Jenski LJ, Stillwell W. Lipid phase separation in phospholipid bilayers and monolayers modeling the plasma membrane. *Biochim. Biophys. Acta* 2001; **1512**: 317–328.
58. Hirai M, Iwase H, Hayakawa T, Koizumi M, Takahashi H. Determination of asymmetric structure of ganglioside-DPPC mixed vesicles using SANS, SAX, and DLS. *Biophys. J.* 2003; **85**: 1600–1610.

 